warwick.ac.uk/lib-publications

Characterisation of carbon nanotube - thermotropic nematic liquid crystal composite materials

O Trushkevych,[14] N Collings,[1] T D Wilkinson,[1] W A Crossland,[1] W I Milne,[1] J Geng,[2] B F G Johnson,[2] and S Macaulay[3]

[1] Cambridge University Engineering Department, Centre for Advanced Photonics and Electronics, 9 J.J. Thomson Ave. Cambridge, CB3 0FA, UK; Tel: 44 1223 748347;

[2] Cambridge University Chemistry Department, Lensfield Road, Cambridge CB2 1EW

[3] Malvern Instruments Ltd, Enigma Business Park, Grovewood Road, Malvern, Worcestershire, WR14 1XZ

Abstract. Dispersions of carbon nanotubes (CNT) in liquid crystals (LC) have attracted a lot of attention due to their unique properties and possible applications in photonics and electronics. However, the dispersions are hard to stabilize, and the doping level in the equilibrium state in LC hosts is vanishingly small. A feedback mechanism of monitoring the quality and doping level in dispersions is required. The characterisation of CNT - water dispersions has been reported, however additional challenges appear in both dispersing and monitoring CNTs in liquid crystals. In this paper we compare different methods of characterising CNT-LC composite materials.

1. Introduction

Nanostructured materials like carbon nanotubes possess remarkable anisotropy. Aligned arrays or dispersions of carbon nanotubes are required in order to benefit from the attractive properties of the individual nanotubes on the macroscopic scale. Carbon nanotubes dispersed in thermotropic nematic liquid crystals may form well aligned systems. [1, 2] Moreover, even small concentration of CNTs in liquid crystals have been shown to lead to large nonlinear optical effects [3-5]. Enhancement of electrooptical [6, 7] as well as electrical and dielectric properties [8] of the LC material have also been reported.

Techniques for dispersing CNTs in aqueous media have been well developed. [9-12] These dispersions are usually stabilized against agglomeration by ions and surfactants [9, 13, 14] or by covalent side wall functionalization [15-17]. Concentrations achievable in such dispersions may be as high as 1% by weight. [9-12] However in liquid crystals the concentrations are very low, especially in equilibrium systems. The currently achievable concentration of CNTs in nematic liquid crystal hosts in a stable dispersion is 10^6 times smaller than the ones quoted for water dispersions.

2. Materials

We have studied SWNTs and MWNTs from various sources (Thomas Swan, Aldrich, CNI, SES, Nanocyl and also those synthesized here at Cambridge University). The liquid crystal hosts were the commercially available materials 5CB, E7, ZLI2222, BLO37 and BLO48 from Merck. Nanotubes were dispersed in nematic liquid crystal hosts using ultrasound for 5 hours at 300W power. Centrifuging is a common step in processing CNT dispersions [9] in order to remove large

---

[4] E-mail or213@cam.ac.uk

agglomerates and bundles of CNTs from the suspension. Alternatively, agglomerates and bundles form residue when left undisturbed for certain time. To ensure a system close to equilibrium we chose natural sedimentation. The mixtures were left undisturbed for at least 2 weeks to eliminate large agglomerates from the suspension.

The dispersions of octadecylamine functionalized SWNTs from Aldrich in E7 required the shortest ultrasonication time (2-4 hours) to obtain uniformly "dark" suspension which also gave longer (~ 2 weeks) sedimentation time. This material was chosen as an example for comparison between different characterisation methods. Depending on the characterisation method, the material was used either in bulk form, on planar membrane filters with 0.2μm pore size, or sandwiched between two glass slides (with transparent ITO electrodes) with planar or homeotropic alignment to form a cell. The thickness of such cells was 20μm and 100μm.

Due to the nature of the dispersing and filtering methods the task of defining the exact concentration of CNTs in solution is far from straightforward. Weighing of substances before mixing does not give reliable information: LC samples are rarely larger than 1g, the limitation of most scales is 0.01mg (giving a minimum measurable percentage by weight (wt %) of 0.001 %). Commercially available CNT materials have purity usually of ~70 - 90% with main impurities in the form of catalyst metal, amorphous carbon and fullerenes. Also, there is a large amount of residue consisting mainly of CNT bundles.

3. Characterisation methods

3.1. *Electron microscopy*
Atomic force microscopy (AFM), environmental scanning electron microscopy (ESEM) and transmission electron microscopy (TEM) can all be used to image individual nanotubes including single wall CNTs. The liquid crystal host may interfere with the imaging by AFM and ESEM. To assess LC - CNT dispersions, Lynch and Patrick [2] suggested the use of planar membrane filters with small pore size, through which the LC - CNT mixture has been filtered, and CNTs remain as a residue. For AFM and ESEM characterisation we used PTFE filters with pore size 0.2 μm.

The above methods are the most informative when a CNT dispersion is to be tested for particle size, concentration, agglomeration, bundling and their alignment in an external electric field. Nevertheless, these methods have a number of limitations including the small area that can be scanned in a time (50 x 50 nm to resolve individual nanotubes), the long time needed to perform one measurement, the difficulty of finding nanotubes if the solution is very dilute, the need to prepare special samples (for AFM and ESEM) and the high cost of equipment.

The precision is good, but CNTs shorter than the filter pore size cannot be registered. Strong flow alignment with the LC may allow nanotubes that are longer than the filter pore size to pass through pores, thus introducing a systematic error.

3.2. *Atomic force microscopy*
Using the octadecylamine functionalized SWNTs in suspensions we have found ~70 individual CNTs or small CNT bundles on 100 μm^2 area of the filter (figure 1a).

The distribution of lengths of the individual or very small bundles of CNTs in the sample is shown on figure 2. The measurement was taken after an initial mixture was deposited on a filter with 0.2μm pore size. Therefore CNTs with a length ≤ 0.2μm could pass through the filter and could not be assessed in this study.

The effective area of the filter was 1.15×10^6 μm^2, and 2 μl of suspension has been filtered through it. Assuming that the distribution of nanotubes is uniform over the filter area, we may estimate a concentration η ~ 4×10^8 particles/ml. This corresponds to having approximately one nanotube or small nanotube bundle per $13.5 \times 13.5 \times 13.5$ μm^3 volume. The volume fraction of CNTs in LC host is $\sim 5 \times 10^{-10}$ or $\sim 5 \times 10^{-9}$ in the case of small bundles rather than individual tubes.

Assuming individually dispersed nanotubes with an average length of 0.5μm and diameter 1.4 nm, the corresponding molecular weight is $M = 1.6 \times 10^6$, and therefore there is $\sim 1.3 \times 10^{-9}$ gram of CNTs in 1 ml of dispersion. The typical density of liquid crystals is ~ 1 g/cm^3, therefore the weight fraction of CNTs is $\sim 10^{-9}$ wt or 10^{-8} wt in the case of small CNT bundles. These figures are an approximation due to assumption made of uniform distribution, and to the fact that we cannot register CNTs smaller than 0.2μm the filter pore size.
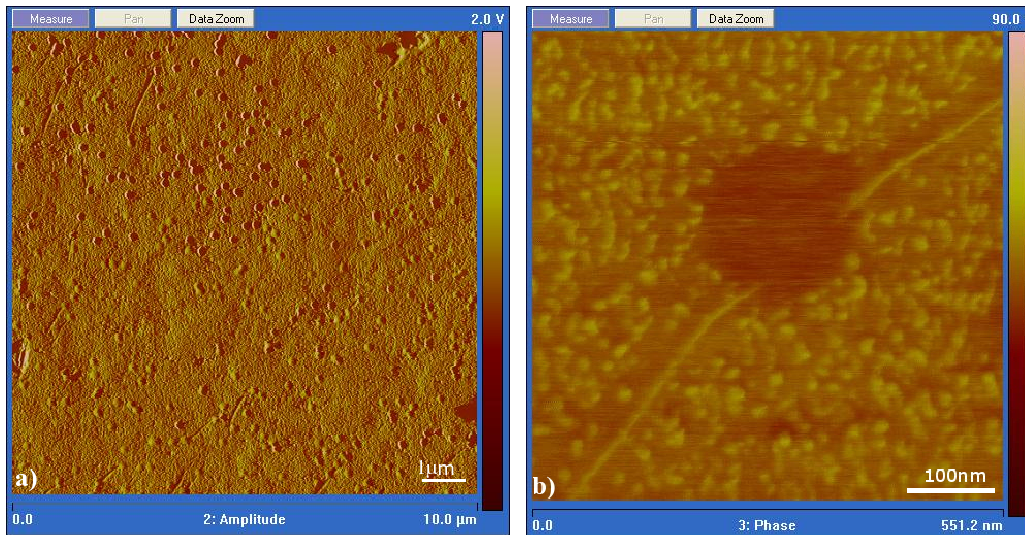
Figure 1 Single walled carbon nanotubes/small bundles on planar filters (pore size 0.2 μm) imaged by AFM.

a) CNTs on filter (round spots are filter pores);

b) individual SWNT seen across a filter pore. Flow alignment and pressure during filtering pulls CNTs into (and possibly through) pores.
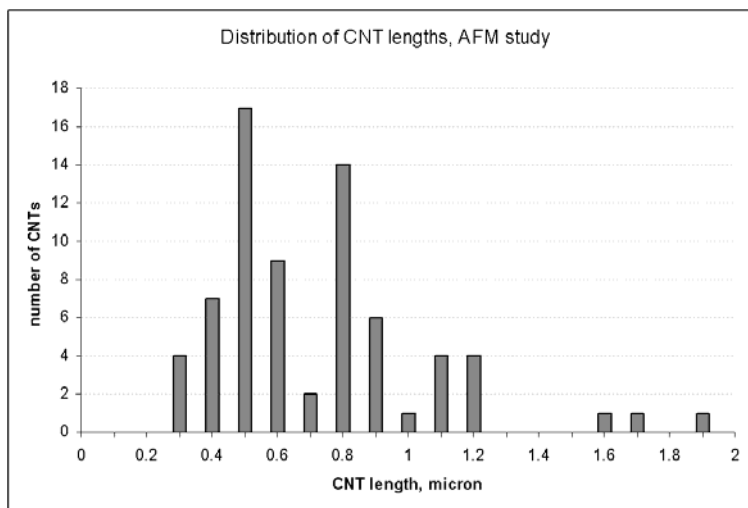
Figure 2. AFM study of the distribution of CNTs by length after 5 hours of sonication at 300W in LC host.

3.3. Environmental Scanning Electron Microscopy

The ESEM system allowed scanning areas as large as 500 μm carbon nanotubes could be clearly seen on the filter through which the suspensions were filtered (figure 3).
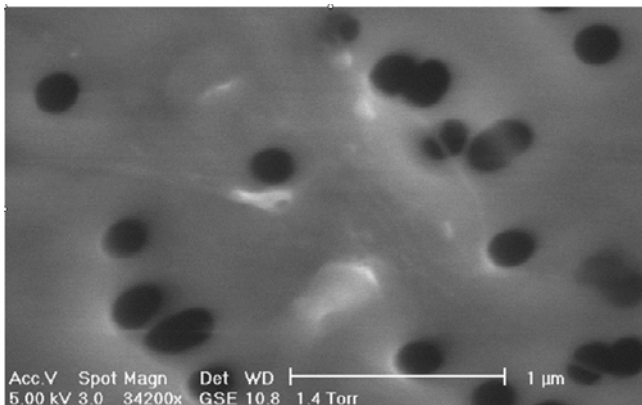
Figure 3 Single-wall CNTs imaged by ESEM technique. The round dots are filter pores.
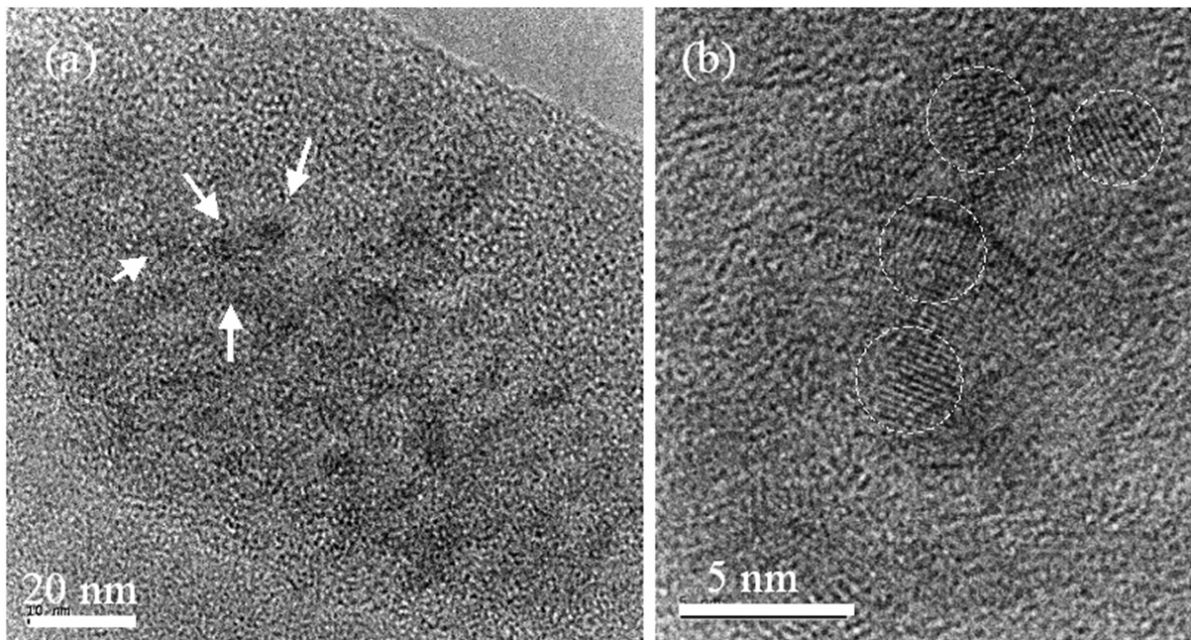
Figure 4 TEM observation of the metal impurities in the octadecylamine functionalized SWNTs – LC (E7) mixture. (a): A low magnification (× 300 k) image shows the metal nanoparticles. (b) A high resolution TEM image (× 800 k) shows the crystalline nature of the particles and the randomly oriented crystal lattices displayed by different nanoparticles (1-3 nm, marked with circles).

### 3.4. Transmission Electron Microscopy

Transmission electron microscopic (TEM) studies were performed with a JEOL JEM-3011 electron microscope operated at 300 kV. To prepare a specimen for the TEM study, a drop of the suspension of the octadecylamine functionalized SWNTs in LC (E7) was deposited on a 400 mesh Cu specimen grid coated with holey carbon film. A freshly prepared suspension was left standing for sedimentation for at least eight weeks to eliminate large agglomerates before it was used to make the TEM sample. It was believed that a thermodynamic equilibrium had been reached in such a suspension. The specimen grid was placed in a sample holder and transferred into the microscope column. Images were recorded at magnifications up to × 800,000.

TEM is usually a powerful means for observing both the morphology and structure of carbon nanotubes. However, in this case no SWNTs could be observed even after some significant effort. This may be not surprising if we consider the very low concentration of SWNTs in the suspension ($\sim 10^{-8}$ - 10^{-9} by weight), and also the special limitations of TEM caused by the small scan area at the high resolutions needed to find the single-walled nanotubes with only a 1-2 nm diameter. Seen areas are typically 50 x 50 nm. Nevertheless, we have observed quite a large number of nanoparticles that are in the suspension (figure 4(a)). These particles are extremely small, typically possessing a diameter of $\sim$1-3 nm. Close inspection using HRTEM revealed that they are single crystals with randomly oriented crystal lattice fringes (figure 4(b)). Almost certainly, these nanoparticles are the catalyst metal used for the growth of the single-walled tubes. This result indicates that although the nanotubes themselves are difficult to find due to their very low concentration in the LC suspension, metal impurities are relatively easier observed using TEM. TEM may be one of the most useful methods to assist in the evaluation of the quality of the SWNTs-LC composite.

3.5. Raman Spectroscopy

The Raman Spectroscopy is an extremely useful and accurate method for studying SWNTs.[18] The method can detect and study even single isolated nanotubes [19, 20]. Raman spectroscopy can be used for CNT characterisation in liquid crystalline matrices [21].

One of the prominent features in Raman spectrum of the CNTs is the radial breathing mode ($\sim$160 - 300 cm^{-1}), associated with a symmetric movement of all carbon atoms in the radial direction. For example, freshly prepared (unstable) suspensions of 0.1 wt % of CNTs in liquid crystalline host have been characterized using the RBM band by Scalia et al [21]. Another strong feature of the CNT Raman spectrum is the G-band ($\sim$1550 - 1590cm^{-1}) however it is very close to the band corresponding to the C-C stretching of aromatic rings in liquid crystal (1606 cm^{-1}) making measurements difficult.

We tested 20μm and 100μm aligned films of CNT doped LCs and also CNT residue on filters[5]. However no CNT specific Raman signal could be detected in our equilibrated LC-CNT dispersions at concentrations of 10^{-9} - 10^{-8} wt.

3.6. Photoluminescence (PL) and PL Confocal microscopy

Photoluminescence spectroscopy[22] and a similar technique widely used in biology called confocal microscopy, may be used as sensitive and informative methods for detecting individually dispersed semiconducting single walled carbon nanotubes. In confocal imaging the light is focused into a single plane of the sample.

When excited in the visible region, semiconducting carbon nanotubes emit in the infra red (900 - >1700nm). The emitted spectrum gives valuable information about the band structure of the CNTs allowing the determination of their diameter, chirality and length. Photoluminescence is suppressed if CNTs are metallic, or if CNTs are bundled together, or if an efficient mechanism of non-radiative energy dissipation exists like energy transfer to the surrounding molecules.

Spectroscopic equipment has the advantage of having a wider range of operating wavelengths and the possibility to integrate the signal over quite large areas, while microscopic techniques may be beneficial when assessing e.g. dispersion uniformity. The limitations of both methods are due to tube bundling. The sensitivity threshold may become an issue in very dilute mixtures.

We have studied 100μm thick cells of CNT doped and undoped liquid crystals and obtained identical results in all these cells. In confocal microscopy the samples were droplets of undoped and CNT doped LCs between microscope slides. The measurements did not show any traces of CNTs.

---

[5] as described above, in the AFM section

The conclusion is that at the 10^{-9} - 10^{-8} wt concentrations, these methods are not suitable.

3.7. Optical microscopy

Large single walled nanotube bundles and multiwalled CNTs and bundles may be directly imaged with a microscope [1]. More importantly, the LC director field may distort around particles or nanostructures and carbon nanotubes in particular [23], and this deformation of the nematic director field may be visible in polarized light, even though the particles (e.g. viruses[24]) may be smaller than the wavelength of visible light.

Extremely low dopant concentrations, as in our case of 1 nanotube or bundle per $13.5 \times 13.5 \times 13.5$ μm^3 volume should therefore be ideal for optical microscopic studies.

We have studied homeotropically aligned undoped and CNT doped LC cells. Undoped samples looked uniformly black under crossed polarizers. The doped cells exhibit visible deformations of the nematic director (bright dots and often crosses) that deform upon electric field application (up to 2MHz frequency). The deformations are likely to be around dopant particles. It is impossible to judge whether those are individual nanotubes or bundles or large agglomerates of nanotubes or impurities.

The cell thickness is 20μm, with homeotropic alignment. The material used was the octadecylamine functionalized CNTs in LC host. The particles are spaced at about 4 - 8μm apart which equals t ~10^9 particles/ml. Assuming the particles are 0.5 μm long nanotubes (as AFM study on this material have shown) and have a diameter of 1.4nm (as specified by the supplier), this gives a volume fraction of $8 \cdot 10^{-10}$ and a weight fraction of $4 \cdot 10^{-9}$ wt (or ~10^{-8} wt for bundles), which is consistent with our calculation of dopant concentration obtained from AFM studies for the same mixture.

From TEM studies we know that the particular CNT-LC dispersion contains metal catalyst nanoparticles (under 5nm in diameter). The agglomerations of these particles may have contributed to the overall particle count and given an overestimated figure for the concentration.

The cross on figure 5b) is due to the fact that the LC director deformation acts as a lens (refractive index change in liquid crystal film).
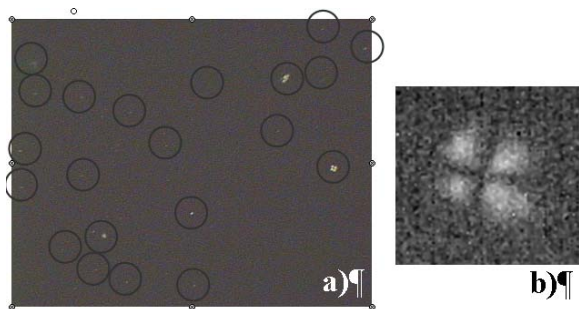

Figure 5 Polarized microscope images of a) CNT-doped LC cell showing some light through the points where the director is deformed. Dark circles mark most noticeable points of deformation. Magnification x50; b) director deformation under crossed polarisers, magnification x200

3.8. Absorption spectroscopy and Fourier spectroscopy

Absorption spectroscopy and Fourier absorption spectroscopy are versatile tools for characterisation of optical materials. CNTs possess strong absorption in the ultraviolet, visible and infrared range. The specific shape of the spectrum depends on the specific CNT material. UV is not convenient for the case of dispersions in liquid crystals, as LCs absorb wavelengths below 360 nm.

Absorption has been used for CNT dispersion characterisation in both films or dispersions in D_2O. [9, 25]

Concentrations $\leq 10^{-8}$ by wt of CNTs are more problematic to study due to their very low absorption. Conventional methods of obtaining good absorption from very dilute absorbing

mixtures rely on long beam path (10 mm) and utilize cuvettes with material in bulk form. This is challenging in the case of liquid crystals. Nematic LC phases in bulk form have non-uniform refractive index and produce strong light scattering. The transparent isotropic (liquid) phase of commercial LC materials is above 70°C (E7), and is now more commonly ~100°C.

On the other hand, liquid crystal materials may be aligned to form uniform films and reduce scattering. Alignment is possible in thin cells (usually 20μm, but may be up to 125μm thick). Such thin cells have extremely low absorption. In addition, the absorption spectrum can be masked by interference between beams reflected from the glass surfaces of a thin cell (the phenomenon commonly used to measure cell thickness).
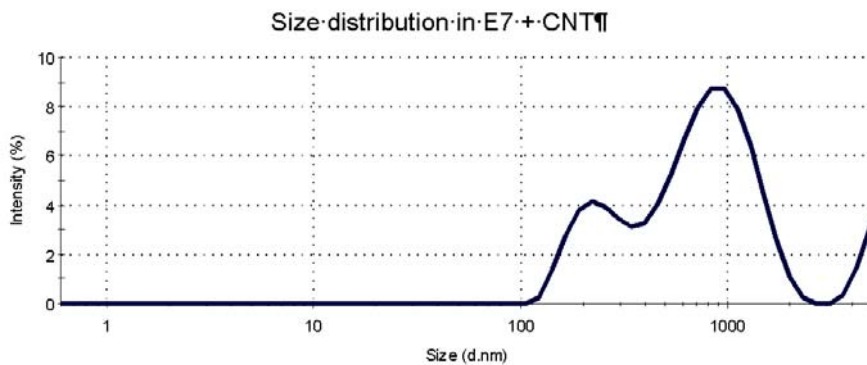

Figure 6 Size distribution of particles in the dispersion of octadecylamine functionalized CNTs (Aldrich) in E7, Dynamic Scattering (Malvern Instruments).

The absence of strong and well defined peaks in the absorption of CNTs limits the use of Fourier absorption spectroscopy which relies on analyzing the spectral frequency domain.

Our estimation (based on measurements on thin LC films and CNT dispersions in D_2O) shows that concentration from absorption measurements can be defined with ~0.2% wt precision when using thin films. When using material in bulk form in the isotropic phase (with an optical path of 10 mm) it would be possible to detect lower concentrations with ~$2 \cdot 10^{-5}$ wt resolution of CNTs. In absorbing planar aligned films precision may be improved when using polarized light, as CNTs have highly anisotropic absorption (dichroism). [26]

3.9. Scattering techniques

There are two main ways of determining particle size distribution in suspensions from the light they scatter. Both rely on measuring the Brownian motion of scattering particles. The translational diffusion coefficient, D, is related to the size of the particles d by the Stokes-Einstein equation:

$$d_h = \frac{kT}{3\pi\eta D}$$

where:

d_h - hydrodynamic diameter of the particle size d; D - translational diffusion coefficient; k - Boltzmann's constant; T - absolute temperature; η - viscosity.

The hydrodynamic diameter refers to how a particle diffuses within a fluid. The translational diffusion coefficient will depend not only on the size of the particle "core", but also on any surface structure, as well as the concentration and type of ions in the medium. All light-scattering particle-sizing techniques have an inherent problem in describing the size of non-spherical particles. If the shape of a particle changes in a way that affects the diffusion speed, then the hydrodynamic size will change. Therefore it is usually much easier to detect small changes in the length of a rod-shaped particle, but not in its diameter.

One technique, Nanoparticle Tracking Analysis (NTA) developed by NanoSight [27] is based on observing scattering from nanoparticles in suspension and analyzing the Brownian motion of each particle. A laser beam is passed through the suspension and scattered light perpendicular to the laser beam is observed through a microscope. The Brownian motion of particles in the field of view is video-recorded using a CCD camera over a period of time (30 s - 5 min), and each particle trajectory is tracked. The information collected about the number and diffusion behaviour of nanoparticles is used to derive their concentration and size distribution. Some implications about non-spherical particle shape may be made from the anisotropy of diffusion of the particle. [27] The minimum detectable size depends on particle refractive index and can be as low as 9-15nm for high refractive index materials such as colloidal silver. The maximum size that can be accurately sized is 1000nm. However larger particles can be observed and counted. For a statistically significant number of particles to be present in the beam, sample concentrations should be above 10^7 particles/ml. Higher concentrations (e.g. 10^8-10^9ml^{-1}) improve measurement accuracy with shorter analysis times. The system resolves even closely sized particles. For carbon nanotube detection, one drawback is that, in one of the dimensions, CNTs are approaching the upper limit of particle size that can be detected. The resulting speckle hampers the measurement.

Pure liquid crystal reference (solution in hexane) gave no scattering with the NanoSight particle tracking system. The ODA functionalized CNT dispersion in LC was measured to have ~$4\cdot10^7$ particles/ml (volume fraction ~$3\cdot10^{-11}$ and weight fraction ~10^{-10} wt) with mean effective hydrodynamic particle size ~200 nm and size distribution 80 – 380nm. All test suspensions were filtered through a 0.45μm filter prior to the investigation.

The dynamic light scattering technique (DLS) also referred to as Photon Correlation Spectroscopy or Quasi-Elastic Light Scattering has been developed by Malvern Instruments[28, 29] to measure particle sizes in suspensions with very a broad dynamic range of sizes from 0.6nm up to 6μm. DLS measures the speed at which the particles are diffusing due to Brownian motion by measuring the rate of fluctuation of the scattered light. This technique benefits from a large statistical selection of data. However, the technique can resolve the sizes of particles only when they have large difference in the size. If size ratio of two particle species is smaller than 3:1, they will show as one species with an intermediate size. There is the possibility of relating scattering results to the concentration of particles, although this has not been implemented in the instrument.

The sensitivity of the system depends on particle size. The smaller the particle, the weaker the scattered signal it produces. The intensity of the signal versus size is proportional to the volume of the particle squared and therefore proportional to the 6th power of its diameter. Therefore, very small particles can be registered only if present at high concentrations or without large particles to mask the signal.

We used particle tracking and dynamic light scattering to study equilibrated LC-CNT mixtures, including the octadecylamine functionalized SWNTs in LC host that was characterized by AFM, TEM and optical microscopy and described above. Mixtures were dissolved in acetone and hexane to suppress scattering due to the nematic phase.

A solution in acetone of E7 liquid crystal (reference) was tested using the DLS system from Malvern and particles ~1.6nm in diameter were detected. This size is consistent with the hydrodynamic diameter of material molecules (0.3 nm x 2 nm) or their parts (acetone may be chemically disrupting the molecules).

A sizeable scattering signal was obtained from doped LCs (however, the concentration was not detected). The measurement of the hydrodynamic diameter of the ODA functionalized nanotubes had two major peaks: around 200nm, and 900 nm (figure 6). Another rise in intensity above 3μm may be due to larger CNT clumps or some other contamination. These peaks have masked a weaker signal from small E7 molecules. Note that the larger the particle, the stronger

the scattering signal it produces. Therefore in this particular system there are more particles with 200nm size than any other ones.[6]

Both measurements are in a good agreement with the AFM studies described above (10^8 particles/ml, 10^{-9} wt, ~500nm CNT length). CNTs have highly anisotropic shape, and their effective diameter is expected to be smaller than their actual length. The larger sized particles detected by DLS may correspond to clumps of nanotubes. They were not detected using the NanoSight technique, because in this case the mixtures were filtered using a 0.45μm pore filter. We did not register any signal from ~5nm catalyst nanoparticles by these two techniques. This is below the resolution limit for the NanoSight tracking system. And in DLS system the signal from larger nanotubes and bundles masked the predictably weak signal from a relatively dilute concentration of ~5nm nanoparticles.

Depolarized dynamic light scattering (DDLS) is similar to DLS, but only the light scattered from anisotropic particles and therefore of different polarization is collected. [10] Detailed studies on CNT dispersions with surfactants in water (0.3wt% concentration) have been reported [10]. The technique allowed monitoring length and diameter of CNT bundles and was used to study the influence of ultrasonication time and power on resulting suspension quality.

Dynamic light scattering and its depolarized version are perhaps the fastest and most sensitive techniques for the given task of assessing the quality of dispersions. They require small samples, but the sample has to be either heated to the isotropic state, or diluted in another solvent to destroy the LC scattering phase. Adding additional solvents makes systems more difficult to analyze, as a strong change in viscosity of the host and potentially lower solubility of CNTs in solvents may lead to CNT aggregation and very poor results even from initially good dispersions.

Other methods of CNT visualization include fluorescent polymer wrapping of carbon nanotubes [30]. Table 1 shows the results of characterisation of the studied E7+CNT system. Table 2 summarizes the discussed characterisation techniques.

Table 1 The results from the different techniques characterising E7 liquid crystal doped with functionalized CNTs from Aldrich.

Method	Concentration	Size	Comment
AFM	10^8 particles/ml (10^{-9} wt)	300 - 1900nm average ~500nm	On filter 0.2μm pore size
Optical microscopy	~10^9 particles/ml ($4 \cdot 10^{-9}$ wt)	n/a	Sizing not possible
Particle tracking (NanoSight)	~$4 \cdot 10^7$ particles/ml (~10^{-10}wt)	~200 nm	In solvent, 0.45μm filter
DLS (Malvern)	n/a but potentially possible	~200nm and ~900 nm	In solvent

Table 2 Techniques for monitoring CNT dispersions.

Method	Sample required	Range	Applicability and limitations

---

[6] From figure 6 the intensity ratio between 200nm and 900nm species is 1:2. This translates to a number density of more than 2000:1 i.e. for each 900nm particle there are 2000 200nm particles.

Method	Sample required	Range	Applicability and limitations
CNT specific			
Raman spectroscopy	LC cell, thin cover glass; on filter	reported studies of 0.1% wt CNT in LC[21]	sensitive to exciting beam polarization signal from CNT may be swamped by LC;
Photoluminescence (PLE) and Confocal microscopy	thin film LC cell, thin cover glass	unknown	CNT bundling quenches luminescence; limited by excitation/readout wavelengths contamination may mask signal
LC specific			
Optical microscopy	LC cell, thin cover glass preferred	min 10^5 particles/ml ($3 \cdot 10^{-13}$ wt), x50 magnification 100μm cell	Contamination must be minimized.
Electron microscopy			
AFM	on filter	~10^5 particles/ml or lower concentrations	particle size must be larger than filter pore size; limited area of scan (50x50μm)[*];
ESEM	on filter	~10^5 particles/ml	limited area of scan (500x500μm)[*]; substrates limit the use of high power beam
TEM	mixture	~10^5 particles/ml	limited area of scan[*], suitable for particles down to 1nm
Spectroscopy (for absorbing dopants)			
Absorption (IR) and FTIR spectroscopy	LC cell (100μm)	~0.2wt%	absorption is too low to be detectable; fringing
	Cuvette, isotropic phase	for 10mm cuvette, ~0.002wt%	needs heating to ~ 70-110˚C
Scattering			
Nanoparticle Tracing Analysis (NanoSight) [27, 31]		min 10^7 particles/ml ($3 \cdot 10^{-11}$wt); size 10 - 1000 nm;	detects concentration, dopant size distribution; limited by number of scattering centres in view
Dynamic light scattering (Malvern) [28, 29]	Cuvette, isotropic phase, solvent	0.6 nm - 6 μm;	detects dopant size distribution; limited by detector sensitivity/ contamination
Depolarized dynamic light scattering		reported studies of 0.3wt% aqueous CNT dispersion[10]	detects anisotropic dopant size and shape; limited by detector sensitivity/ contamination

[*] area of scan should be no larger than 50 × 50 nm to resolve individual nanotubes

4. Conclusions

We have explored various possibilities of characterising CNT-LC dispersions. We have achieved ~10^{-9}wt doping level in equillibrated mixtures. The characterisation methods may be classified into the following groups: CNT specific (Photoluminescence, Raman), LC specific (optical microscopy), Spectroscopy, Electron microscopy and Scattering techniques.

Four methods were found to be suitable for characterising the achievable concentrations of CNTs in LC. These methods are AFM, optical microscopy, Particle Tracking (NanoSight) and Dynamic Light Scattering (Malvern). The results obtained from these methods are consistent. The most sensitive and comprehensive method is AFM, however it is technically difficult. The fastest and simplest are the methods based on scattering. Optical microscopy is also convenient and informative, however it does not provide direct information about the size of the particles and is sensitive to any contamination.

5. Acknowledgements

6. References

[1]   Dierking I, Scalia G, Morales P, LeClere D. Aligning and reorienting carbon nanotubes with nematic liquid crystals. Advanced Materials. 2004;16(11):865-9.

[2]   Lynch MD, Patrick DL. Organizing Carbon Nanotubes with Liquid Crystals. Nano Letters. 2002 November 13, 2002;2(11):1197-201.

[3]   Khoo IC, Ding J, Zhang Y, Chen K, Diaz A. Supra-nonlinear photorefractive response of single-walled carbon nanotube- and C60-doped nematic liquid crystal. Applied Physics Letters. 2003;82(21):3587-9.

[4]   Lee W, Chiu C-S. Observation of self-diffraction by gratings in nematic liquid crystals doped with carbon nanotubes. Optics Letters. 2001;26(8):521-3.

[5]   Trushkevych O, Collings N, Crossland PWA, Wilkinson TD, Georgiou A, Milne WI. Projection of holograms from photorefractive optically addressed spatial light modulators. Journal of Nonlinear Optical Physics & Materials. 2007;16(3).

[6]   Huang C-Y, Hu C-Y, Pan H-C, Lo K-Y. Electrooptical Responses of Carbon Nanotube-Doped Liquid Crystal Devices. Japanese Journal of Applied Physics. 2005;44(11):8077-81.

[7]   Lee W, Wang C-Y, Shih Y-C. Effects of carbon nanosolids on the electro-optical properties of a twisted nematic liquid-crystal host. Applied Physics Letters. 2004;85(4):513-5.

[8]   Chen H-Y, Lee W. Suppression of field screening in nematic liquid crystals by carbon nanotubes. Applied Physics Letters. 2006;88(22):222105-3.

[9]   Rozhin AG, Scardaci V, Wang F, Hennrich F, White IH, Milne WI, et al. Generation of ultra-fast laser pulses using nanotube mode-lockers. Physica Status Solidi (B). 2006;243(13):3551-5.

[10]   Badaire S, Poulin P, Maugey M, Zakri C. In situ measurements of nanotube dimensions in suspensions by depolarised dynamic light scattering. Langmuir. 2004;20:10367-70.

[11]   Sabba Y, Thomas EL. High-Concentration Dispersion of Single-Wall Carbon Nanotubes. Macromolecules. 2004 June 29;37(13):4815-20.

[12]   Huang YY, Ahir SV, Terentjev EM. Dispersion rheology of carbon nanotubes in a polymer matrix. Physical Review B (Condensed Matter and Materials Physics). 2006;73(12):125422.

[13]   Lagerwall JFP, Scalia G, Haluska M, Dettlaff-Weglikowska U, Giesselmann F, Roth S. Simultaneous alignment and dispersion of carbon nanotubes with lyotropic liquid crystals. Physica Status Solidi (B). 2006;243(13):3046-9.

[14]   Moore VC, Strano MS, Haroz EH, Hauge RH, Smalley RE, Schmidt J, et al. Individually Suspended Single-Walled Carbon Nanotubes in Various Surfactants. Nano Letters. 2003;3(10):1379-82.

[15]   Tagmatarchis N, Prato M. Functionalization of carbon nanotubes via 1,3-dipolar cycloadditions. Journal of Materials Chemistry. 2004;14:437 - 9.

[16]   Torre Gdl, Blau W, Torres T. A survey of the functionalization of single-walled nanotubes. The chemical attachment of phtalocyanine moieties. Nanotechnology. 2003;14:765-71.

[17]   Kumar S, Bisoyi HK. Discotic-functionalized carbon nanotubes and their insertion into a columnar matrix. *21st International Liquid Crystal Conference*. Keystone, Colorado, USA 2006.

[18]   Zhao Q, Wagner HD. Raman spectroscopy of carbon nanotube-based composites. Philosophical Transactions of Royal Society Lond A. 2004;362:2407 - 24.

[19]   Dresselhaus MS, Dresselhaus G, Jorio A, Souza Filho AG, Saito R. Raman spectroscopy on isolated single wall carbon nanotubes. Carbon. 2002;40(12):2043-61.

[20]   Dresselhaus MS, Jorio A, Souza Filho AG, Dresselhaus G, Saito R. Raman spectroscopy on one isolated carbon nanotube. Physica B: Condensed Matter. 2002;323(1-4):15-20.

[21]   Scalia G, Haluska M, Dettlaff-Weglikowska U, Giesselmann F, Roth S. Polarized Raman spectroscopy study of SWNT orientational order in an aligning liquid crystalline matrix. *Electronic Properties of Novel Nanostructures, XIX International Winterschool/Euroconference on Electronic Properties of Novel Materials* American Institute of Physics 2005:114-7.

[22]   O'Connel MJ, Bachilo SM, Huffman CB, Moore VC, Strano MS, Haroz E, et al. Band Gap Fluorescence from Individual Single-Walled Carbon Nanotubes Science. 2002;297:593.

[23]   Dodge R, Kang S-W, Kumar S, Park C, Siochi M. Carbon nanotube liquid crystal composites. The american Physical Society Meeting MAR06; 2006; 2006.

[24]   Jang C-H, Cheng L-L, Olsen CW, Abbott NL. Anchoring of Nematic Liquid Crystals on Viruses with Different Envelope Structures. Nano Letters. 2006;6(5):1053-8.

[25]   Lebedkin S, Arnold K, Hennrich F, Krupke R, Renker B, Kappes MM. FTIR-luminescence mapping of dispersed single-walled carbon nanotubes. New Journal of Physics. 2003;5:140.1 - .11.

[26]   Ichida M, Mizuno S, Kataura H, Achiba Y, Nakamura A. Anisotropic optical properties of mechanically aligned single-walled carbon nanotubes in polymer. Applied Physics A. 2004;78 1117-20.
[27]   Robert Carr, Diaper T, Barrett E. NanoParticle Tracking Analysis – The Halo™ system. *Particulate Systems Analysis 2005*. Stratford-upon-Avon, UK: Royal Society of Chemistry 2005.
[28]   Malvern_Instruments_Ltd. 2006 [cited; Available from: http://www.malvern.com/
[29]   Nobbmann U, Kaszuba M. Nanoparticle Size Characterisation. *Malvern Instruments Seminar*. Cambridge, UK 2007.
[30]   Didenko VV, Moore VC, Baskin DS, Smalley RE. Visualization of Individual Single-Walled Carbon Nanotubes by Fluorescent Polymer Wrapping. Nano Letters. 2005 August 10, 2005;5(8):1563-7.
[31]   NanoSight. www.nanosight.co.uk. [cited; Available from: